Crystal Structure of Picotpaulite, TlFe$_2$S$_3$, from Allchar, FYR Macedonia

Tonči Balić-Žunić,[1],* Ljiljana Karanović[2] and Dejan Poleti[3]

[1] *Department of Geography and Geology, University of Copenhagen, Øster Voldgade 10, DK-1350 Copenhagen K, Denmark.*

[2] *Laboratory of Crystallography, Faculty of Mining and Geology, Đušina 7, 11000 Belgrade, Serbia*

[3] *Department of General and Inorganic Chemistry, Faculty of Technology and Metallurgy, Karnegijeva 4, 11000 Belgrade, Serbia*

* *Corresponding author: E-mail: tonci @geo.ku.dk*

Received: 10-03-2008

Dedicated to the memory of Professor Ljubo Golič

Abstract

The crystal structure of the mineral picotpaulite, TlFe$_2$S$_3$, was solved and refined using single-crystal X-ray diffraction data collected at room temperature. The symmetry is orthorhombic, space group *Cmcm*, with unit-cell parameters: a = 9.083(6), b = 10.754(6), c = 5.412(4) Å, V = 528.6(6) Å^3, Z = 4. The structure was refined to the conventional *R* factor 0.0532 for 226 independent reflections with $I > 2\sigma(I)$ and 21 variables. Picotpaulite is isostructural with minerals rasvumite (KFe$_2$S$_3$) and pautovite (CsFe$_2$S$_3$), as well as with a number of synthetic compounds belonging to the CsCu$_2$Cl$_3$ structure type. The structure consists of double chains of FeS$_4$-tetrahedra running along [001] interconnected by TlS$_{10}$ coordination polyhedra, which form zig-zag chains along the same direction. The Fe–Fe distances between neighbours along the chain direction and perpendicular to it are 2.706(2) and 2.693(6) Å, respectively, indicating strong Fe–Fe interactions. The average oxidation state of Fe is +2.5, achieved by electron transfer over the close Fe sites. Thallium coordination polyhedron can be described as a combination of a square antiprism adjacent to a trigonal prism. The $6s^2$ electrons of Tl behave as an inert pair and the atom is situated in the centroid of its coordination.

Keywords: Picotpaulite, crystal structure, mixed valence, Fe–Fe interactions, electron delocalization, s^2 inert pair.

1. Introduction

Picotpaulite was originally described some forty years ago from the world-known locality of rare Tl minerals, Allchar, FYR Macedonia.[1] The mineral was found in realgar and in association with pyrite, lorandite and raguinite. However, its crystal structure was not determined. This paper presents a single-crystal X-ray diffraction study and structure solution on a sample of picotpaulite from the type deposit (Allchar) and its relation to minerals rasvumite and pautovite, as well as to some synthetic isostructural compounds.

Both isostructural minerals, rasvumite (KFe$_2$S$_3$) and recently described pautovite (CsFe$_2$S$_3$), are from the Kola Peninsula, Russia. Rasvumite is from the Khibina massif[2] and pautovite is from the Palitra peralkaline pegmatite, Kedykverpakhk Mountain, Lovozero alkaline complex.[3] Numerous isostructural synthetic compounds are known as well:

– mixed-valence thioferrates AFe$_2$S$_3$ with A = Ba^{2+}, K$^+$, Rb$^+$ and Cs^{+};[4–6]
– rubidium and caesium iron chalcogenides AFe$_2$Y$_3$ with A = Rb$^+$, Cs$^+$ and Y = Se^{2-}, Te^{2-};[7]
– rubidium and caesium copper halides ACu$_2$X$_3$ with A = Rb$^+$, Cs$^+$ and X = Cl-, Br-, I -.[8–13]

2. Experimental

Due to a perfect cleavage and plasticity of the mineral, it was very difficult to separate a suitable fragment for the X-ray study from the sample, which consisted of bundles of elongated black crystals up to 2.5 mm long (Fig. 1). Finally, by covering a larger irregular needle by nail-polish it was possible to cut off an usable fragment while the glue was still slightly viscous. The obtained fragment was a lath $0.03 \times 0.07 \times 0.44$ mm in size with faces parallel to {010}, {100}, and {001}, respectively, and only slightly bent on its ends. The diffraction spots were visibly elongated and distorted, but it was still possible by a careful refinement of the crystal lattice orientation and choice of the integration volume in reciprocal space to obtain usable intensities of reflections for a structure solution and refinement.

Room-temperature data were collected on a Bruker-AXS four-circle diffractometer with a Smart 1000CCD detector and a flat graphite monochromator, using MoKa radiation ($\lambda = 0.71073$ Å) from a fine-focus sealed X-ray tube. The sample-to-detector distance and collimator size were 38.7 and 0.5 mm, respectively. The software *SMART* was used for data collection, *SAINT* for integration of intensities and *Lp* correction. The absorption effects were corrected by a combination of face-indexed (program *XPREP* from the *SHELXTL* package) and multi-scan met-

Fig. 1. A group of picotpaulite crystals, from which a fragment was isolated for the crystal structure analysis. The elongated habit, perfect cleavage and pronounced plastic deformation can be seen. The approximate dimensions of the field of view are 3×3.5 mm.

hod (program *SADABS*). This approach significantly decreased R_{int} value from 0.30 to 0.08. All software is produced by Bruker-AXS.

The structure was solved by direct methods[14] and refined using full-matrix least-squares on F^2 and the *SHELXL97* software[15] implemented in the *WinGX* system

Table 1. Crystal data and some details of the structure refinement for picotpaulite.

Formula	TlFe$_2$S$_3$
Crystal size (mm)	$0.03 \times 0.07 \times 0.44$
Absorption correction factors	$T_{min} = 0.022$, $T_{max} = 0.405$
Data measurement temperature (K)	298(1)
Crystal description	black lath-shaped fragment
Formula weight, M_r	412.25
Crystal system, space group (No.)	orthorhombic, *Cmcm* (63)
a (Å)	9.083(6)
b (Å)	10.754(6)
c (Å)	5.412(4)
V (Å^3)	528.6(6)
Z	4
D_x (g cm^{-3})	5.180
μ (mm^{-1})	36.84
$F(000)$	724
Range for data collection, θ (°)	*4.49 - 25.02*
Range of Miller indices	$-10 \le h \le 10$ $-12 \le k \le 12$ $-6 \le l \le 6$
Reflections collected / unique	1934 / 274 ($R_{int} = 0.083$)
Reflections / restraints / parameters	274 / 0 / 21
Observed reflections [$I > 2\sigma(I)$]	226
Extinction coefficient, k $^+$	0.0004(8)
Goodness-of-fit, S	1.125
R indices [$I > 2\sigma(I)$]	R$_1$ = 0.0532, wR$_2$ = 0.1310 $^{++}$
R indices (all data)	R$_1$ = 0.0663, wR$_2$ = 0.1429 $^{++}$
$(\Delta/\sigma)_{max}$	< 0.0001
Largest difference peak and hole (e Å^{-3})	$\Delta\rho_{max} = 4.60$, $\Delta\rho_{min} = -2.21$

$^+$ $F_c^* = F_c k[1+0.001F_c^2\lambda^3/\sin(2\theta)]^{-1/4}$
$^{++}$ $w = 1/[\sigma^2(F_o^2) + (0.0848\,P)^2 + 16.9765P]$ where $P = (F_o^2 + 2F_c^2)/3$

Table 2. Atomic coordinates, equivalent isotropic[+] and anisotropic[++] displacement parameters (Å^2) for picotpaulite.

Atom	x	y	z	U_{eq}	U_{11}	U_{22}	U_{33}	U_{23}	U_{13}	U_{12}
Tl	0.5	0.1609(2)	0.25	0.0448(8)	0.045(1)	0.060(1)	0.029(1)	0	0	0
Fe	0.3518(3)	0.5	0	0.0203(9)	0.020(2)	0.037(2)	0.004(1)	–0.001(1)	0	0
S1	0.5	0.6212(7)	0.25	0.019(2)	0.022(4)	0.028(4)	0.008(3)	0	0	0
S2	0.2191(7)	0.3827(6)	0.25	0.028(1)	0.025(3)	0.046(3)	0.014(2)	0	0	–0.013(2)

$^{+}$ U_{eq} is defined as one third of the trace of the orthogonalized U_{ij} tensor.
$^{++}$ The anisotropic displacement factor exponent takes the form: $-2\pi^2[h^2a^{*2}U_{11} + ... + 2hka*b*U_{12}]$.

of programs.[16] The highest and the lowest residuals in the final ΔF map were centred on Tl. Further crystal and refinement details can be found in Table 1. The final atomic parameters are listed in Table 2.
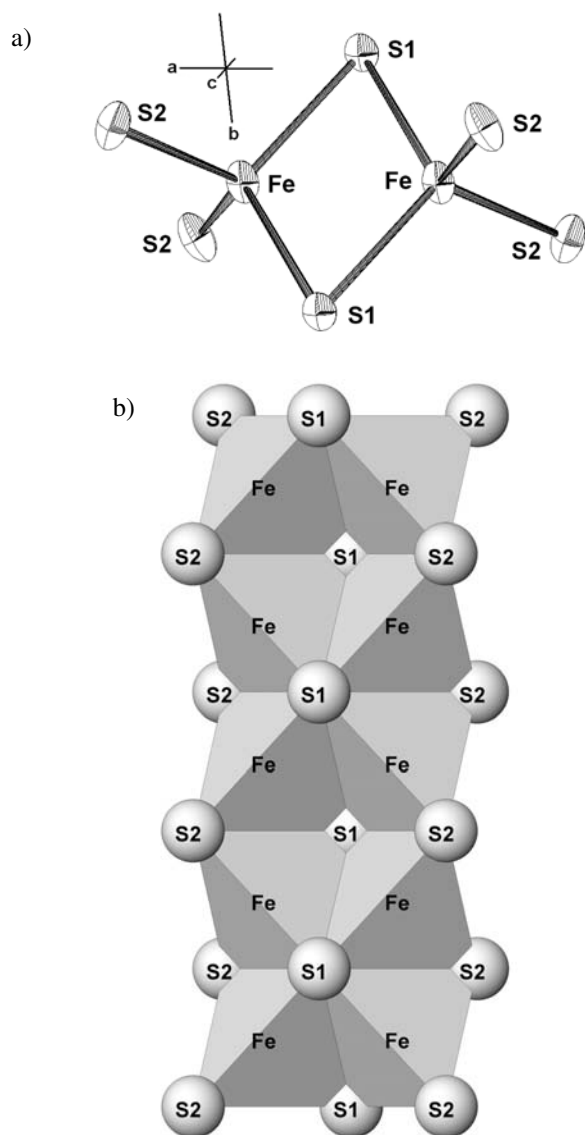
a)

b)

Fig. 2. (a) The pairs of tetrahedra with the atomic numbering scheme (displacement ellipsoids at 50 % probability level), and (b) the double chains of FeS$_4$-tetrahedra in picotpaulite as viewed approximately along [010] (*a*-axis horisontal, *c*-axis vertical).

3. Results and Discussion

3. 1. Description of the Structure

The core of the complex Fe polysulfide anions in picotpaulite are planar [Fe$_2$S$_2$] clusters, which contain two Fe atoms bridged by two S1 atoms. These cores are terminated by four S2 atoms. Two S1 and two S2 atoms are
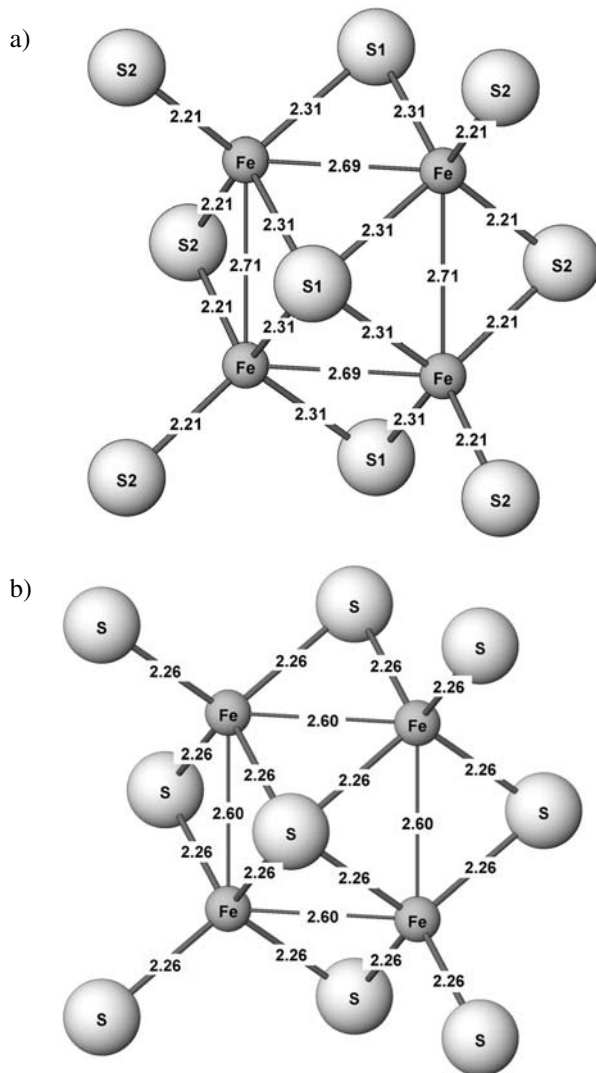
a)

b)

Fig. 3. Part of the chains of FeS$_4$-tetrahedra in picotpaulite (a), and corresponding part of sheets in mackinawite (b).

bonded to one Fe atom forming a slightly distorted tetrahedron (Fig. 2a).

The tetrahedra pairs sharing S1–S1 edges are placed in the planes parallel to (100) and are further interconnected to infinite linear double chains by sharing S1–S2 edges positioned close to planes parallel to (001), as shown in Fig. 2b. The double chains running parallel to [001] are responsible for the pronounced columnar to needle-like habit of the mineral. Identical double chains were found in rasvumite and other isostructural compounds. In related mackinawite (FeS) structure,[17,18] edge-sharing FeS₄-tetrahedra are further polymerized in infinite sheets and each iron is bonded to four equidistant sulphur atoms (Fig. 3).

The bond distances and angles of picotpaulite are given in Table 3. Similar to rasvumite, in picotpaulite three tetrahedral S–Fe–S angles [108.8(2), 106.3(2), 110.8(2) °] are close to the ideal value (109.5 °), but the fourth one (S2–Fe–S2) is larger and has the value of 113.8(3)°. The four sulphur atoms form an almost perfect tetrahedron, as can be seen from a negligible volume distortion calculated according to Makovicky and Balić-Žunić[19], which amounts to only 0.2% (Table 4). The same holds true for all other isostructural compounds. The difference in bonding angles is mostly due to the displacement of Fe atom from the centre of the tetrahedron towards the unshared S2–S2 edge, reflected in eccentricity, which is the largest distortion parameter of the coordination polyhedron (Table 4). The symmetry of the Fe site and its coordination polyhedron is 2 (C_2), which puts the two Fe atoms from a [Fe₂S₂] cluster on a common two-fold axis. As can be seen from Table 3, the differences in the lengths of the tetrahedral edges arising from the difference to the ideal tetrahedral symmetry result in a variation from the shortest S1–S2 edges of 3.62 Å to the longest S1–S1 edge of 3.76 Å. It is interesting that the shortest edge is between the

Fe–Fe neighbours along the *c*-axis, whereas the longest one lies between the Fe–Fe pairs of [Fe₂S₂] cluster, which runs across the chain (Fig. 3).

As in other isostructural compounds, the large cation (A = Tl) is bonded to ten S atoms (Fig. 4a). The site symmetry of the Tl atom and of its coordination polyhedron is $m2m$ (C_{2v}). The coordination polyhedron can be described as containing two adjacent parts: a square antiprism (housing the eight shortest bonds) and a trigonal prism sharing one of the lateral faces with one square base of the antiprism (Fig. 4a). Tl atom is situated almost perfectly in the ideal centre of the coordination. The calculated displacement is less than 0.001 Å.

Tl-polyhedra are interconnected in zigzag chains extending along [001], where every Tl-polyhedron shares two rectangular faces of the trigonal-prism part with neighbouring polyhedra. (Fig. 4b).

The lath-like morphology of picotpaulite crystals and the perfect cleavage along the two pinacoids: {010} and {100}, where the former one predominates, can be explained by the distribution of Tl–S bonds. The four shortest Tl–S bonds [3.392(4) Å] connect the Fe–S chains to form slabs parallel to {010}. The remaining Tl–S bonds are longer (>3.49 Å) and more easily disrupted. A very easy plastic deformation and bending of needles obtained by cleavage is also understandable from the character of Tl–S bonding. Gliding of Fe–S chains relative to each other should be relatively easily accomplished by recombination of Tl–S bonds, which must be very weak because of their length and the high Tl coordination number.

An interesting aspect of the crystal structure is the packing of the large atoms (S and Tl). Sulphur and thallium atoms are arranged in a cubic eutaxy (Fig. 5). The eutactic planes, parallel to (221), are composed of double rows of sulphur atoms running parallel to [-110] and in-

Table 3. The coordination tables of cations for picotpaulite. The bold numbers in the diagonals are the bond distances (Å), the numbers above the diagonal the bond angles (°), and the numbers below the diagonal the ligand-ligand distances (Å).

Tl

	S2	S2	S2	S2	S2	S2	S1	S1	S2	S2
S2	**3.392 (4)**	164.1 (2)	105.9 (2)	71.9 (2)	121.5 (2)	70.5 (2)	133.9 (1)	59.2 (1)	63.9 (2)	102.1 (2)
S2	6.718 (6)	**3.392 (4)**	71.9 (2)	105.9 (2)	70.5 (2)	121.5 (2)	59.2 (1)	133.9 (1)	102.1 (2)	63.9 (2)
S2	5.412 (4)	3.980 (9)	**3.392 (4)**	164.1 (2)	121.5 (2)	70.5 (2)	59.2 (1)	133.9 (1)	63.9 (2)	102.1 (2)
S2	3.980 (9)	5.412 (4)	6.718 (6)	**3.392 (4)**	70.5 (2)	121.5 (2)	133.9 (1)	59.2 (1)	102.1 (2)	63.9 (2)
S2	6.008 (8)	3.973 (7)	6.008 (8)	3.973 (7)	**3.493 (7)**	93.8 (2)	63.4 (1)	63.4 (1)	166.7 (2)	99.4 (2)
S2	3.973 (7)	6.008 (8)	3.973 (7)	6.008 (8)	5.103(10)	**3.493 (7)**	63.4 (1)	63.4 (1)	99.4 (2)	166.7 (2)
S1	6.415 (6)	3.445 (9)	3.445 (9)	6.415 (6)	3.719 (5)	3.719 (5)	**3.580 (5)**	98.2 (1)	123.0 (1)	123.0 (1)
S1	3.445 (9)	6.415 (6)	6.415 (6)	3.445 (9)	3.719 (5)	3.719 (5)	5.412 (4)	**3.580 (5)**	123.0 (1)	123.0 (1)
S2	3.700 (6)	5.434 (8)	3.700 (6)	5.434 (8)	7.038(10)	5.406(10)	6.304 (9)	6.304 (9)	**3.593 (7)**	67.3 (2)
S2	5.434 (8)	3.700 (6)	5.434 (8)	3.700 (6)	5.406(10)	7.038(10)	6.304 (9)	6.304 (9)	3.980 (9)	**3.593 (7)**

Fe

	S2	S2	S1	S1
S2	**2.208(5)**	113.8(3)	106.3(2)	110.8(2)
S2	3.700(6)	**2.208(5)**	110.8(2)	106.3(2)
S1	3.618(8)	3.719(5)	**2.311(5)**	108.8(2)
S1	3.719(5)	3.618(8)	3.757(8)	**2.311(5)**

Table 4. Some bond distances (Å) and coordination parameters for cations in isostructural AB_2X_3 compounds.*

Coumpound	A cation (CN 10)						B cation (CN 4)									Reference
	$\langle d\rangle$ (Å)	V_P (Å³)	VD	EC	AS	BV	$\langle d\rangle$ (Å)	V_P (Å³)	VD	EC	BV	B–X1 distance	B–X2 distance	B–B distance across chains	B–B distance along chains	
$BaFe_2S_3$	3.46(25)	84.6(3)	0.092	0.074	0.058	1.81	2.28(1)	6.04(4)	0.002	0.006	2.92	2.285(6)	2.269(7)	2.698(5)	2.643(1)	4
$TlFe_2S_3$	3.49(9)	86.4(4)	0.092	<0.001	0.026	0.75	2.26(6)	5.90(8)	0.002	0.041	3.09	2.311(5)	2.208(5)	2.692(4)	2.706(2)	Present study
KFe_2S_3	3.52(11)	88.8(4)	0.090	0.017	0.031	0.85	2.26(7)	5.95(8)	0.003	0.046	3.05	2.325(4)	2.206(4)	2.711(4)	2.716(2)	2
$RbFe_2S_3$	3.58(12)	93.4(3)	0.092	0.021	0.031	0.97	2.27(7)	5.99(3)	0.003	0.050	3.00	2.335(6)	2.208(5)	2.716(5)	2.723(1)	5
$CsFe_2S_3$	3.68(11)	101.5(4)	0.092	0.019	0.028	1.23	2.28(6)	6.04(4)	0.004	0.051	2.96	2.343(7)	2.212(7)	2.700(7)	2.741(1)	5
$RbFe_2Se_3$	3.68(13)	101.5(2)	0.092	0.020	0.033	1.00	2.38(6)	6.94(4)	0.003	0.051	3.05	2.439(3)	2.329(3)	2.765(5)	2.819(1)	7
$CsFe_2Se_3$	3.77(12)	109.2(4)	0.095	0.016	0.030	1.22	2.39(6)	7.04(7)	0.003	0.038	2.95	2.446(6)	2.345(6)	2.767(10)	2.837(1)	7
$RbFe_2Te_3$	3.91(16)	121.2(5)	0.097	0.019	0.040	0.93	2.57(4)	8.68(14)	0.007	0.024	3.59	2.606(2)	2.537(2)	2.821(4)	2.961(1)	7
$CsCu_2Cl_3$	3.71(22)	104.1(2)	0.090	0.063	0.048	0.96	2.39(12)	6.92(2)	0.001	0.076	0.97	2.490(3)	2.284(4)	3.113(4)	2.800(1)	10
$RbCu_2Br_3$	3.77(33)	110.3(1)	0.091	0.091	0.069	0.86	2.50(9)	7.90(1)	0.004	0.053	1.04	2.573(2)	2.421(2)	3.243(3)	2.776(1)	13
$CsCu_2Br_3$	3.84(22)	115.5(2)	0.093	0.055	0.048	1.03	2.51(9)	8.04(3)	0.001	0.058	1.02	2.587(5)	2.425(4)	3.094(7)	2.909(1)	10
$CsCu_2ClI_2$	3.95(23)	125.9(14)	0.092	0.028	0.055	1.13	2.59(11)	8.87(32)	0.006	0.064	1.05	2.682(6)	2.498(7)	3.068(13)	2.960(5)	11
$RbCu_2I_3$	4.02(37)	133.6(5)	0.093	0.087	0.079	0.88	2.65(7)	9.47(11)	0.008	0.040	1.07	2.716(3)	2.592(4)	3.426(5)	2.864(2)	12
$CsCu_2I_3$	4.06(23)	136.6(6)	0.094	0.045	0.052	1.07	2.65(5)	9.49(15)	0.002	0.032	1.08	2.694(2)	2.599(2)	3.131(5)	3.036(2)	9

* $\langle d\rangle$ = average bond distance, V_P = volume of the coordination polyhedron, VD = volume distortion, EC = eccentricity, AS = asphericity (for CN 4 it is 0 by definition), BV = valence sum from bond valence calculations. All parameters are calculated by program IVTON.[32] For the calculation of bond valences the parameters of Brese and O'Keeffe[33] were used.
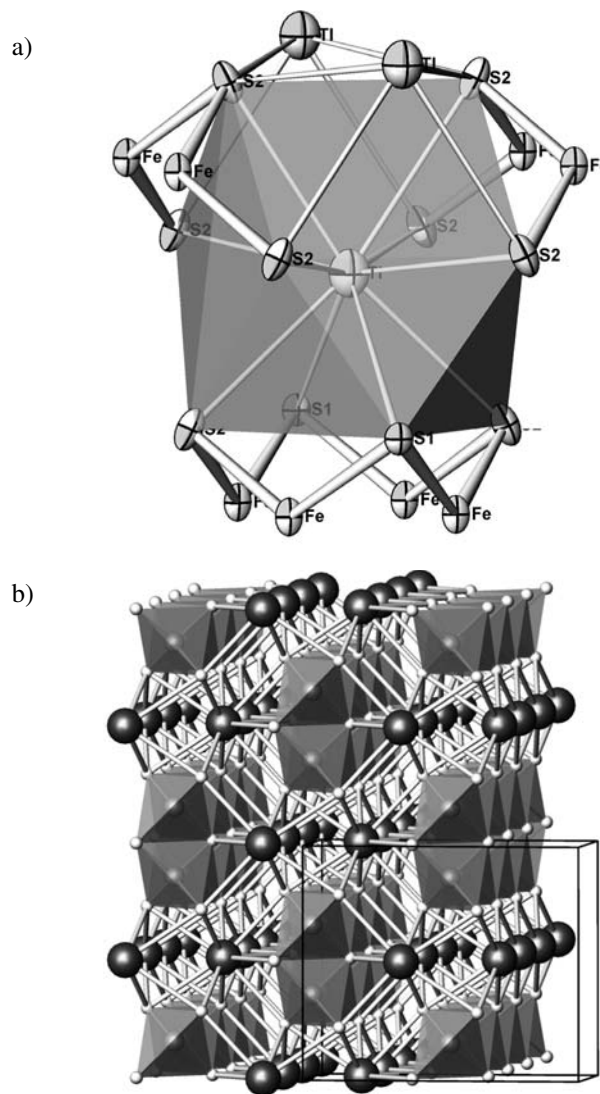
a)

b)

Fig. 4. (a) The coordination polyhedron of Tl atom (*b*-axis vertical). The symmetry planes are vertical and pass through two Tl and two S2 atoms at the top, respectively. S atoms in the lower part of the coordination polyhedron build a square antiprism, those in the upper part a lying trigonal prism. With the addition of the two closest Tl atoms, a cuboctahedral surrounding, characteristic for cubic eutaxy, is completed (see text and Fig. 5). (b) The crystal structure of picotpaulite viewed approximately along [001] (*a*-axis vertical). The largest dark spheres represent Tl atoms. Fe coordination tetrahedra are shaded.

terchanging with double mixed Tl–S rows. One quarter of available tetrahedral interstices is filled by Fe atoms.

Iron coordination tetrahedra, which have bases in the same layer, are arranged in groups of four with two apices up and two down (Fig. 5). In eutaxy, each Tl and S1
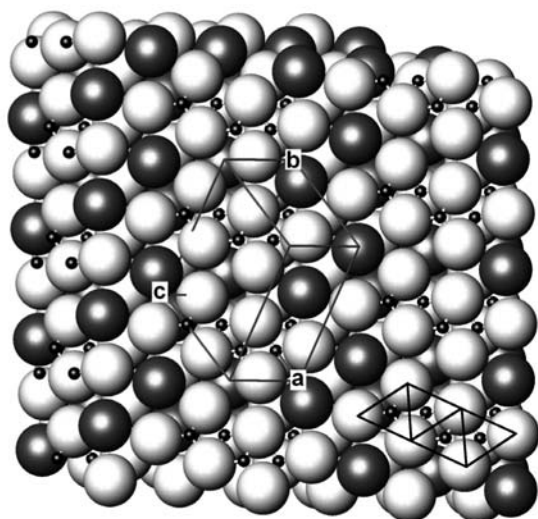
Fig. 5. The crystal structure of picotpaulite represented as a cubic eutaxy of large (S light and Tl dark) atoms with layers parallel to (221). Fe atoms represented as small black spheres. One unit cell with the orientation of crystal axes is indicated. In the lower right corner the bases of the four adjacent occupied tetrahedral holes associated with the uppermost layer are indicated.

have ten S and two Tl neighbours, whereas S2 has eight S and four Tl neighbours. As typical for the cubic eutaxy, the surrounding eutactic atoms form a cuboctahedron.

As a measure of discrepancy of the arrangement from an ideal eutaxy, volume discrepancies of the surrounding atoms from an ideal cuboctahedron can be used. Using the centroid of coordination[20] the volumes of circumscribed spheres around the coordination cuboctahedra of Tl, S1 and S2 can be calculated as 198.5, 202.4, and 201.0 Å^3, respectively, whereas the polyhedral volumes are 109.6, 114.7, and 111.5 Å^3, respectively. V_s/V_p ratio for a regular cuboctaheron is $[4/5(2)^{1/2}]\pi = 1.7772$. The values for Tl, S1, and S2 are 1.8111, 1.7646, and 1.8027, respectively, which gives +2%, –1%, and +1% volume discrepancy from an ideal cuboctahedron as defined by Makovicky and Balić-Žunić.[19] Furthermore, the atoms in a perfect eutaxy lie in the centroids of their surroundings, and the surrounding atoms lie on the surface of the common sphere. Calculating the discrepancies from this ideal situation, one obtains 9%, 3% and 4%, respectively, as the values of eccentricities, whereas the asphericities amount to 9%, 2% and 5%, respectively. As can be seen, all distortion parameters show that the arrangement deviates by less than 10% from an ideal cubic eutaxy.

3. 2. Comparison With Similar Structures

Among the family of thioferrates isostructural with picotpaulite different valence states of iron are expected for BaFe$_2$S$_3$ and the rest of the group. According to stoichiometry, the former should contain Fe(II) and the rest a

mixture of Fe(II) and Fe(III). The Mössbauer-spectroscopy study of synthetic rasvumite, KFe$_2$S$_3$[21] showed a presence of only one type of Fe, in accordance with the crystal structure study, with characteristics intermediate to Fe(II) and Fe(III). At the same time, the spectroscopical

$$s_{\text{Fe–S}} = 179.7 \sum_i R_i^{-6.81} \qquad (1)$$

characteristics are very similar to those observed for Fe in BaFe$_2$S$_3$.[22] The geometrical characteristics of Fe are indeed very similar in all structures (Table 4) and do not show variations expected from the differences in Fe valence. The bond-valence calculations according to the formula suggested by Brown and Altermatt[23] predict for all cases Fe(III), contrary both to stoichiometry and the Mössbauer measurements. Closer to reality are the results of calculation according to the empirical bonding equation 1 where R_i is the bond distance, suggested by Hoggins and Steinfink[24] for metal-iron-sulphide compounds. The formula gives 2.77 for the valence of Fe in picotpaulite and 2.63 for Fe in BaFe$_2$S$_3$, emphasizing again the discrepancy between the geometrical parameters and the expected stoichiometry of the latter compound.

The expected Fe^{3+}–S, (Fe^{2+}/Fe^{3+})–S and Fe^{2+}–S bond distances are 2.26, 2.31 and 2.36 Å, respectively.[25] In K$_3$Fe$_2$S$_4$[26] and mineral sternbergite, AgFe$_2$S$_3$,[27] there are single tetrahedral FeS$_2$ chains with +2.5 as a formal oxidation state of Fe ions. The observed average Fe–S and Fe–Fe distances are 2.31 and 2.84 Å, respectively, for Fe$_2$K$_3$S$_4$ and 2.28 and 2.76 Å, respectively, for sternbergite. In picotpaulite the corresponding average distances are 2.26 and 2.70 Å, respectively, and they are very close to the average distances for the whole AFe$_2$S$_3$ series containing double chains (Table 4). Finally, in mackinawite, with FeS$_4$-tetrahedra interconnected in infinite sheets (Fig. 3) the equivalent values are 2.26 Å for Fe–S and 2.60 Å for Fe–Fe distance. Therefore, an increase in the polymerization of tetrahedra is accompanied by a decrease of both Fe–S and Fe–Fe distances, and this increases a possibility for electron delocalization.

It can be concluded that the double chains in picotpaulite and isostructural thioferrates represent relatively rigid units stabilized by Fe–Fe interactions. The electronic structure of the units enables combination with large cations of various oxidation states, with a maintenance of the same character of bonding. In the case of structures with monovalent large cations, the electron transfer is necessary just for the achievement of the stabilizing mixed-valence character of Fe. However, in the case of BaFe$_2$S$_3$ the close Fe–Fe contacts are supposed to accommodate surplus valence electrons. Reiff et al.[22] have determined a very low electrical resistivity for BaFe$_2$S$_3$ (0.5 Ω cm in average at room temperature) and a high anisotropy of the property, with resistivity parallel to the c-axis being about ten times lower than that perpendicular to the c-axis. This

effect can be explained by the delocalization of a part of electrons through the network of Fe–Fe bonds.

One can observe small dissimilarities in the geometry of Fe coordinations between $BaFe_2S_3$ and the rest of the isostructural thioferrates. The small distortions of the coordination tetrahedra are reflected in different lengths of the S1–S1 and S2–S2 edges (Fig. 2). In $BaFe_2S_3$ the former is shorter than the latter, which lies on the border of the tetrahedral rows. In other thioferrates, the opposite is true. In $BaFe_2S_3$ iron atoms are situated almost perfectly in the centres of their coordination polyhedra and all bonds are almost equal in length, whereas other structures show a larger eccentricity of Fe atoms, which are displaced away from the central chain line and S1–S1 edges. Fe–Fe distances along the chain extension are shorter than those perpendicular to it in $BaFe_2S_3$, whereas the opposite situation can be observed for other thioferrates. Expressed similarity in the geometrical parameters of all Fe–S chains suggests, however, an unique bonding and electron-band structure, so the small differences are probably a consequence of a partial filling of the conduction band, which can be assumed for $BaFe_2S_3$.

All of these crystal chemical characteristics also are found in the selenoferrates and teluroferrate (Table 4). Quite a different situation can be seen with Cu as the tetrahedral cation. In accordance with the stoichiometry the valence state is Cu(I) and the bond distances are as expected, what can be seen from the results of the bond valence calculations (Table 4). The Cu–Cu distances are significantly longer than Fe–Fe and more sensitive to the type of the additional cation in the structure. The eccentricities of Cu atoms diminish with the increase of the anion size, which suggests that the eccentricity is a consequence of the cation-cation repulsion (Table 4).

It is interesting that the same binuclear iron-sulphur cores containing planar Fe_2S_2 or more complicated clusters like those found in picotpaulite and other thioferrates, are also building blocks in some complex biological molecules. As the structural parts of many enzymes, ferredoxins and other iron-sulphur proteins, the valence-delocalized $[Fe^{2+}Fe^{3+}]$ clusters are of great interest in molecular biology because of their role as active sites in electron transfer reactions.[28,29] The proteins containing iron-sulphur active sites are present in all organisms and function as catalytic centres and mediators in complex redox systems, in which the iron-sulphide ions have variable formal oxidation states: $[Fe_2S_2]^0$, $[Fe_2S_2]^+$ and $[Fe_2S_2]^{2+}$, which correspond to the presence of $2Fe^{2+}$, $Fe^{2+} + Fe^{3+}$ and $2Fe^{3+}$ ions, respectively.[30,31]

The relationship between the size of A cation and unit cell parameters of thioferrates is shown in Fig. 6. One can see that a nearly linear relationship exists for the K, Rb and Cs compounds. In $BaFe_2S_3$ the values deviate very much from this trend, especially for the *b* and *c* parameter. The former is much longer, the latter much shorter than predicted from the K–Rb–Cs trend. The differences can
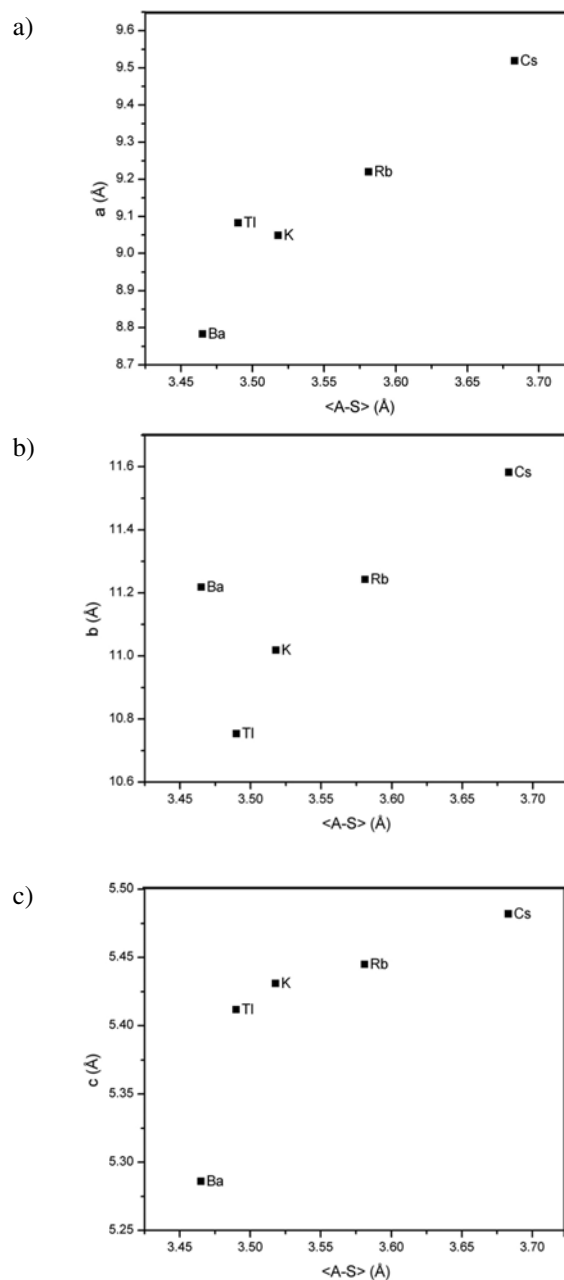

Fig. 6. The relationships between the unit-cell parameters and the A–S average bond distances in AFe_2S_3 compounds. For literature see Table 4. The estimated standard deviations correspond in size to the symbols.

be explained as an influence of the character of Fe_2S_3 chains. Generally, the size of the A cation influences *c* parameter the least, because it depends on the stretching of the relatively rigid chains. The other two depend on the chain separation.

As mentioned earlier, the bonding pattern in Fe_2S_3 chains in the barium compound can be supposed to include a significant electron delocalization along the chains with a consequent shortening of the Fe–Fe distances in

this direction. To adapt to the size of the A cation, the structure must at the same time accommodate an increased separation between the chains, and it happens predominantly along the *b* axis direction. This is reflected also in the relatively large eccentricity of Ba, compared to other A atoms (Table 4). Due to the symmetry of the coordination polyhedron, the eccentricity is a consequence of the displacement of the A atom from the centre of coordination along the *b* axis.

Very interesting is that Tl also deviates from the K–Rb–Cs trend, especially as regards *a* and *b* parameters. As mentioned earlier, Tl shows by far the smallest eccentricity. Tl^+ contains the $6s^2$ lone electron pair, which is often considered a cause for stereochemically distorted coordinations. In this structure $6s^2$ must be an inert pair and it is not displaced from the centre of the Tl atom. It is difficult to find the reasons for this behaviour from the geometric parameters alone. Sitting in the centre of the ten-fold coordination means that Tl atoms are moved closer into the spaces that separate the Fe_2S_3 chains along the *a* axis (see Fig. 4) compared to other A atoms, which are somewhat displaced from the centre of coordination. This is the reason why picotpaulite achieves longer *a* and shorter *b* parameter than expected from the K–Rb–Cs trend in Fig. 6.

Regardless of the type of the A cation, all AX_{10}-polyhedra show practically the same volume distortion, which is equal to 9% volume deficit compared to the maximum volume polyhedron of the same coordination number and with the same size of the circumscribed sphere. The same values are obtained for all thioferrates and thiocuprates isostructural with picotpaulite. This shows that in this structure type the shape of the polyhedron depends on the packing conditions of anions, which is rather uniform, and not so much on the type of the A atom.

4. Conclusion

The mineral picotpaulite ($TlFe_2S_3$) adopts the Cs-Cu_2Cl_3 structure type. Picotpaulite is isostructural with minerals rasvumite (KFe_2S_3) and pautovite ($CsFe_2S_3$), as well as with a number of synthetic compounds. The structure of picotpaulite can also be described as an eutactic structure, *i.e.* sulphur and thallium atoms are arranged in a cubic eutaxy with one quarter of available tetrahedral interstices filled by small Fe atoms. The distortion parameters show that the arrangement deviates by less than 10% from an ideal cubic eutaxy.

Comparative analysis of the Fe coordinations in picotpaulite and isostructural thioferrates supports a mixed valence $Fe^{2.5+}$ state with a delocalization of the part of the 3*d* electrons enabled by the short Fe–Fe distances. Fe–S bond lengths are consistent in all thioferrates of this structure type and correspond to the usual Fe^{3+}–S values, which is not in accordance with their stoichiometry. The increase in the polymerization of FeS_4-tetrahedra is ac-

companied by a decrease of both Fe–S and Fe–Fe distances, and this increases a possibility for electron delocalization.

The lone electron pair of Tl behaves surprisingly as a completely inert pair in the strucutre of picotpaulite and Tl exhibits more regular coordination than the large cations without lone electron pairs which can be observed in this structure type.

6. References

1. Z. Johan, R. Pierrot, H.-J. Schubnel, F. Permingeat, *Bull. Soc. Franc. Mineral. Cristallogr.* **1970**, *93*, 545–549.
2. J. R. Clark, G. E. Brown, *Am. Mineral.* **1980**, *65*, 477–482.
3. I. V. Pekov, A. A. Agakhanov, M. M. Boldyreva, V. G. Grishin, *Can. Mineral.* **2005**, *43*, 965–972.
4. H. Y. Hong, H. Steinfink, *J. Solid State Chem.* **1972**, *5*, 93–104.
5. R. H. Mitchell, K. C. Ross, E. G. Potter, *J. Solid State Chem.* **2004**, *177*, 1867–1872.
6. M. Reissner, W. Steiner, J. Wernisch, H. Boller, *Hyperfine Interact.* **2006**, *169*, 1301–1304.
7. K. O. Klepp, W. Sparlink, H. Boller, *J. Alloys Compd.* **1996**, *238*, 1–5.
8. C. Brink, N. F. Binnendijk, J. Van de Linde, *Acta Cryst.* **1954**, *7*, 176–180.
9. N. Jouini, L. Guen, M. Tournoux, *Rev. Chim. Mineral.* **1980**, *17*, 486–491.
10. G. Meyer, *Z. Anorg. Allg. Chem.* **1984**, *515*, 127–132.
11. S. Geller, J. M. Gaines, *J. Solid State Chem.* **1985**, *59*, 116–122.
12. K. P. Bigalke, A. Hans, H. Hartl, *Z. Anorg. Allg. Chem.* **1988**, *563*, 96–104.
13. S. Hull, P. Berastegui, *J. Solid State Chem.* **2004**, *177*, 3156–3173.
14. G. M. Sheldrick, *SHELXS97*, University of Göttingen, Germany, **1997a.**
15. G. M. Sheldrick, *SHELXL97*, University of Göttingen, Germany, **1997b.**
16. L. J. Farrugia, *J. Appl. Cryst.* **1999**, *32*, 837–838.
17. A. R. Lennie, S. A. T. Redfern, P. F. Schofield, D. J. Vaughan, *Mineral. Mag.* **1995**, *59*, 677–683.
18. M. Wolthers, S. J. Vaan der Gaast, D. Rickard, *Am. Mineral.* **2003**, *88*, 2007–2015.

19. E. Makovicky, T. Balić-Žunić, *Acta Cryst.* **1998,** *B54,* 766–773.

20. T. Balić-Žunić, E. Makovicky, *Acta Cryst.* **1996,** *B52,* 78–81.

21. G. Amthauer, K. Bente, *Naturwissenschaften* **1983,** *70,* 146–147.

22. W. M. Reiff, I. E. Grey, A. Fan, Z. Eliezer, H. Steinfink, *J. Solid State Chem.* **1975,** *13,* 32–49.

23. I. D. Brown, D. Altermatt, *Acta Cryst.* **1985,** *B41,* 244–247.

24. J. T. Hoggins, H. Steinfink, *Inorg. Chem.* **1976,** *15,* 1682–1685.

25. R. D. Shannon, "Bond distances in sulfides and preliminary tables of sulfide crystal radii: – in Structure and Bonding in Crystals" Vol. 2, Academic Press, New York, pp. 53–70 **1981.**

26. W. Bronger, U. Ruschewitz, P. Mueller, *J. Alloy. Compd.* **1995,** *218,* 22–27.

27. F. Pertlik, *N. Jb. Miner. Monat.* **1987,** 458–464.

28. R. H. Holm, P. Kennepohl, E. I. Solomon, *Chem. Rev.* **1996,** *96,* 2239–2314.

29. A. Fish, D. Tsafi, O. Itzhak, N. Rachel, L. Oded, *J. Mol. Biol.* **2005,** *350,* 599–608.

30. B. R. Crouse, J. Meyer, M. K. Johnson, *J. Inorg. Biochem.* **1995,** *59,* 536–536.

31. H. Beinert, R. H. Holm, E. Münck, *Science* **1997,** *277,* 653–659.

32. T. Balić-Žunić, I. Vicković, *J. Appl. Cryst.* **1996,** *29,* 305–306.

33. N. E. Brese, M. O'Keeffe, *Acta Cryst.* **1991,** *B47,* 192–197.

Povzetek

Pri sobni temperaturi je bila z metodo rentgenske strukturne analize na monokristalih narejena kristalna struktura minerala pikotpaulita, $TlFe_2S_3$. Spojina kristalizira v ortorombski prostorski skupini Cmcm z a = 9.083(6), b = 10.754(6), c = 5.412(4) Å, V = 528.6(6) Å³ in Z = 4. Pikotpaulit je izostrukturen z mineraloma razvumitom (KFe_2S_3) in s pautovitom ($CsFe_2S_3$) in z vrsto spojin, ki spadajo k $CsCu_2Cl_3$ strukturnemu tipu. V strukturi so dvojne verige FeS_4-tetraedrov, ki so medseboj povezane s TlS_{10} koordinacijskimi poliedri.